

Evidence for Dual Pathway in Through-Space Singlet Energy Transfers in Flexible Cofacial Bisorphyrin Dyads

Grégory Pognon,^[a] Jennifer A. Wytko,^[a] Pierre D. Harvey,^{*[b]} and Jean Weiss^{*[a]}

Abstract: Flexible “pacman” scaffolds built upon a calix[4]arene platform bearing a [18]crown-6 ether and either two OH functions or two OPr groups at the lower rim have been used to generate donor–acceptor (D–A) dyads incorporating a zinc–porphyrin donor and a free-base porphyrin acceptor. Through-space singlet energy transfer (SET) in the D–A dyads was studied by time-resolved fluorescence spectroscopy. Although the effects of conformational changes are well documented when the chromophores switch from a non-cofacial to a cofacial arrangement, little is known about flexible pacman scaffolds in which the changes are lim-

ited to the distance between the chromophores. The known SET rates for reported, geometrically well-defined, rigid pacman D–A dyads were used as calibration to estimate the D–A distances in the flexible pacman dyads. Due to the flexibility of the calix[4]arene spacer, the D–A dyads adopt a “closed” or “open” geometry that is tuned by intramolecular hydrogen bonds (O–H...[18]crown-6 ether) and by solvent interactions. Changes in the SET rates between the open and closed

geometries were surprisingly less dramatic than expected, and are explained by a dual SET pathway that is specific to the calix[4]arene platform. Time-resolved fluorescence studies support the hypothesis that, for the “open” conformer, the preferred through space SET pathway (i.e., at the shortest distance) is located within the calix[4]arene cavity through the cofacial phenyl groups. For the “closed” conformer, the preferred through space SET route is located between the zinc and free-base porphyrins.

Keywords: calixarenes • energy transfer • porphyrinoids • zinc

Introduction

The structural resolution of the special pair involved in the primary events in photosynthesis^[1] has generated great interest in cofacial bisorphyrin architectures.^[2] Among the variety of bisorphyrin scaffolds reported, rigid pillared bisorphyrins have proven to be an excellent tool for the mechanistic study of the distance dependence of singlet and triplet energy transfer (ET).^[3,4] In particular, critical interchromo-

phore separation for a dominant Dexter or Förster ET mechanism has been established. Rigid scaffolds have been used to force the quasi-cofacial bischromophore arrangement, and, hence, to control the intermacrocyclic spacing in photoactive pacman bisorphyrins. Although flexible porphyrin dimers and their potential use as sensing devices have been reported,^[5] their structures lacked cofacial preorganisation.^[6] Conformational switching of spacers such as bipyridine^[7] and terpyridine moieties has been used to interconvert a non-cofacial to a cofacial bisorphyrin arrangement, providing potential sensing of metals bound to the polyimine site.^[8] Recently, the advantages of flexible calix[4]arene spacers that control either cofacial or slipped dimer bisorphyrin species have been demonstrated.^[9–13] Calixarene spacers provide flexibility to porphyrin dimers within a given topography, leading to switchable conformers and controlled molecular motions. So far, species containing identical chromophores have been used for redox induced tuning of the porphyrins’ spacing in the pacman (cofacial) arrangement,^[10,11] or for thermal geometry tuning in a slipped dimer arrangement.^[12] As suggested by recent reports using resorcinarenes,^[14] or calix[4]arenes,^[15] there is much to expect

[a] Dr. G. Pognon, Dr. J. A. Wytko, Dr. J. Weiss
Institut de Chimie
UMR 7177 CNRS-Université Louis Pasteur
4 rue Blaise Pascal, BP. 1032, 67070 Strasbourg (France)
Fax: (+33)90-24-14-31
E-mail: jweiss@chimie.u-strasbg.fr

[b] Prof. Dr. P. D. Harvey
Département de Chimie, Université de Sherbrooke
2500, boul. de l’Université, Sherbrooke
Québec, J1K 2R (Canada)
Fax: (+1)819-821-8017
E-mail: Pierre.Harvey@USherbrooke.ca

Supporting information for this article is available on the WWW under <http://dx.doi.org/10.1002/chem.200800299>.

from through-space interactions between photo- or electroactive species in tunable systems that allow the detection of small geometry changes within a unique, fixed cone conformation.

The first flexible pacman bisporphyrin generation comprising cofacial bis-tetraarylporphyrins organised around a calixarene platform showed that only weak excitonic interactions were observed between the two porphyrins, despite the use of frozen cone or 1,3-alternate conformations.^[9] To shorten the distance between the two tetrapyrrolic macrocycles, two major structural modifications were introduced in the design of more compact scaffolds. First, the steric hindrance at the porphyrin periphery was reduced by using octaethylporphyrin (OEP) moieties instead of tetraarylporphyrins. Second, the rigid linker that couples the motion of the calixarene platform to the porphyrins was shortened from a phenylethynyl to a simple ethynyl function. Together, these changes decreased the porphyrin–porphyrin distance without drastically increasing the steric hindrance about the calixarene's wide rim. The synthetic availability of the compact scaffolds **1** and **2** makes them extremely attractive for the generation of photochemical dyads, given that hetero bisporphyrin species can be obtained.

A series of flexible pacman homo-bisporphyrins and donor–acceptor (D–A) dyads (Figure 1) and their efficiencies of energy transfer are reported. Whereas scaffolds of type **1** can theoretically exist in three typical calixarene conformations, namely partial cone, 1,3-alternate and cone, pacman compounds of type **2** can only exist in the cone conformation owing to the presence of both the crown ether and the propyl substituents. Figure 2 depicts ball and stick representations of MM2-minimised geometries of calixarenes bearing two ethynyl substituents at the wide rim. Figure 2a corresponds to a vertically flattened calixarene cone in which the two aromatic rings bearing the porphyrins are parallel, providing the shortest inter-chromophore distance (closed pacman). The second geometry (Figure 2b) corresponds to a horizontally flattened calixarene cone in which the two aromatic rings bearing the crown ether are roughly parallel. The presence of hydrogen bonding pinches the calixarene's narrow rim and pushes the ethynyl groups apart, creating a large dihedral angle between the two porphyrin planes (open pacman). The third geometry (Figure 2c) is a partial cone in which the spacing between the aromatic rings bearing the ethynyl porphyrins is similar to the distance in the flattened cone in Figure 2a; however, the non-cofacial arrangement of the chromophores (Figure 2c) restores free rotation about the ethynyl linker for any substituent opposite the crown ether.

The upper and lower limits of the distance separating the two anchoring groups for porphyrins are also indicated in

Figure 2. These distances were estimated from calculations and confirmed by data from X-ray structures available in the literature. Based on the reported solid-state structure of a peralkylated calixarene bis(NiOEP) complex, the lower limit for the distance between the two ethynyl–OEP planes is 3.25 Å.^[10] For a tetraalkylated species, the maximum distance between the ethynyl-substituted *meso*-carbon atoms of the two porphyrins would be around 8 Å. This distance is consistent with X-ray data reported in the literature for calixarene–diethynyl gold(I) complexes.^[16] For hydrogen-bonded dialkylated analogues in the cone conformation (Figure 2b), the two *meso*-carbon atoms of the porphyrin would be approximately 12 to 15 Å apart, because hydrogen bonding pulls the hydroxyl groups towards the crown ether groups. The predicted distance between *meso*-carbon atoms is consistent with solid-state data,^[17] and also with calculated geometries^[18] reported by Swager for a calixarene actuator.^[15] Finally, for a dialkylated type **1** pacman scaffold in a partial cone conformation, the two anchoring points for the

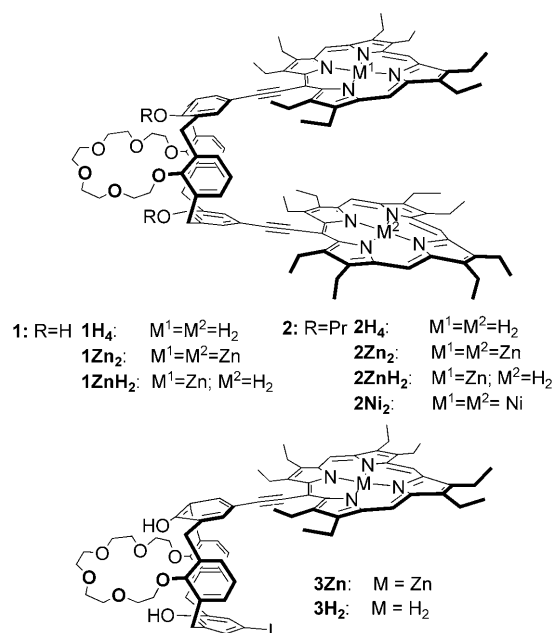


Figure 1. Free-base, mono- and di-zinc species of pacman scaffolds **1** and **2**, and synthetic intermediates.

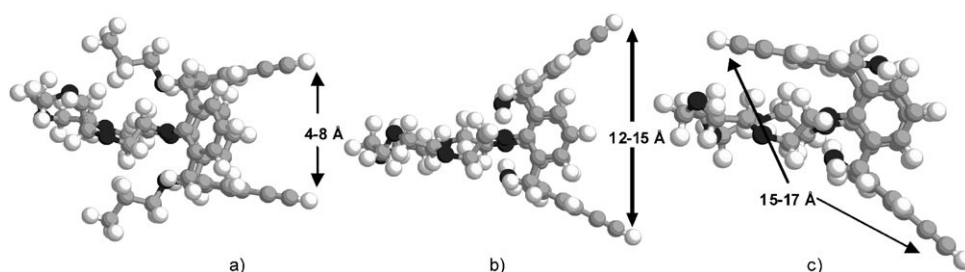


Figure 2. Representation of a) a peralkylated (scaffold **2**) cone calix[4]arene or b) cone and c) partial cone dialkylated (scaffold **1**) calix[4]arene and lower and upper distances (in Å) between the anchoring points for each porphyrin at the end of the ethynyl substituents based on literature data.^[10,11,14–18]

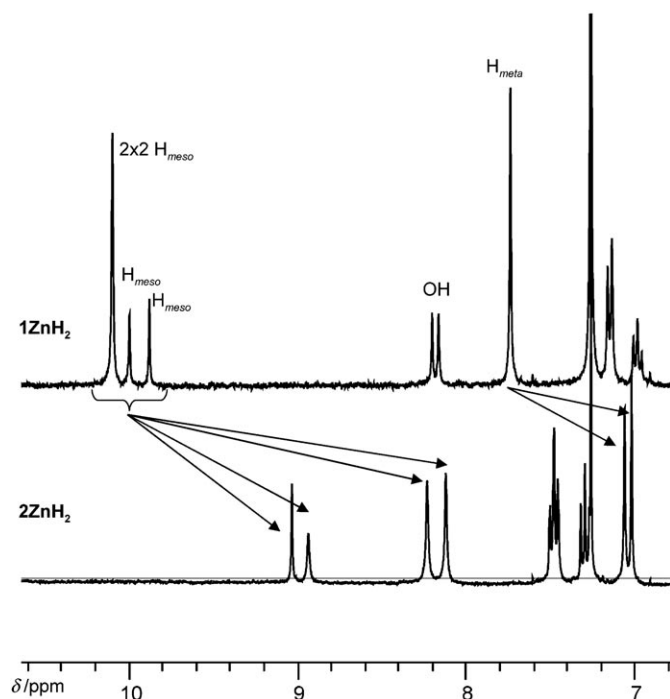


Figure 3. Aromatic region of ^1H NMR spectra of 1ZnH_2 and 2ZnH_2 in CDCl_3 at 298 K (300 MHz).

porphyrins point in opposite directions and would be separated by approximately 15–17 Å, as shown in Figure 2c.

The rate of singlet–singlet energy transfer in flexible pacman bisporphyrins might be controlled by easily addressable geometric changes in the spacer's conformation. However, in calixarene pacman scaffolds, the conjugated nature of the bridge between the chromophores and the spacer renders this analysis more complicated than expected. Indeed, singlet energy transfer rates and efficiencies were examined and assigned not only to different conformers of the calixarene spacer, but also to different energy-transfer pathways within the pacman architectures. A hypothesis is provided concerning the preferred pathway of the fast, through-space, singlet–singlet energy transfer, which may occur either directly between the porphyrins in a closed pacman geometry or through interactions inside the cavity of the spacer in the open conformer.^[2,19]

Results and Discussion

Synthesis and characterisation: The free-base bisporphyrin 1H_4 (Figure 1) was synthesised using the conventional Sonogashira coupling procedure of the corresponding diiodo calixcrown-6 derivative with 5-ethynyl-octaethyl metalloporphyrins, based on previously developed methodology.^[10,13] A non-selective metallation^[4] of 1H_4 and 2H_4 with one equivalent of zinc(II) generated both the bis-zinc derivatives 1Zn_2 and 2Zn_2 and the zinc/free-base energy dyads 1ZnH_2 and 2ZnH_2 in statistical yields. By successive purification and re-

cycling of the bis-zinc species, through regeneration of the corresponding free bases, the dyads were prepared on a reasonable scale.

Figure 3 compares the aromatic region of the ^1H NMR spectra for the two dyads 1ZnH_2 and 2ZnH_2 . In the latter, a significant shielding is observed for the porphyrins' *meso* protons and the calixarene's *meta* protons of the aromatic ring bearing the ethynyl linkage. The comparison illustrates that the introduction of propyl groups on the lower rim of the calixarene spacer forces the pacman structure to close and brings the two porphyrin rings closer to each other. Upon metallation, no spectral changes were observed for 1Zn_2 , 1ZnH_2 , 2Zn_2 and 2ZnH_2 compared to their bis(free-base) counterparts. The absence of changes in the chemical shifts, especially those of the porphyrins' *meso* protons, indicates that the metallation of the porphyrin core has no influence on the pacman conformation (see Figure S1 in Supporting Information). The exclusive presence of a cone conformation is unambiguously deduced by the simple AX pattern for the calixarene's methylene bridges at $\delta=3.4$ and 4.7 ppm (see Experimental Section). For pacman 1ZnH_2 , the chemical shifts of the porphyrin rings are very similar to those observed for isolated ethynyl OEPs. Thus, the predominance of a persistent open geometry for pacman **1** in non-protic organic solvents can be deduced from ^1H NMR data. It is also reasonable to assume that in the dominant closed geometry of the per-alkylated pacman **2**, the distance between the porphyrins is shorter than in the open conformation of pacman **1**.

For a more reliable estimation of the porphyrin–porphyrin distance in scaffolds of type **2**, the binding of guests such as diazabicyclooctane (DABCO) and C_{60} fullerene was investigated. UV/Vis titration of 2Zn_2 with DABCO in dichloromethane (see Figure S2 in the Supporting Information) yielded a $\log K_a=6.39\pm0.05$ for a 1:1 2Zn_2 /DABCO complex. This value is two orders of magnitude lower than those observed in previously reported, more flexible cofacial species.^[6,9,10,20–22] However, the formation of a 1:1 complex corresponds to DABCO binding within the tweezers, confirming that the porphyrin–porphyrin distance in the pacman scaffold **2** in organic solvents is approximately 7 Å and is probably smaller in the absence of this guest, as shown by the upfield shifts of the porphyrin signals in the ^1H NMR spectrum. The nitrogen–nitrogen distance in DABCO is approximately 2.7 Å, to which a reported nitrogen–zinc coordination bond of 2.1 Å needs to be added twice^[23] to give a zinc–zinc distance of 6.9 Å in the DABCO bound receptor 2Zn_2 . Pentacoordinated zinc is expected to come out of the porphyrin plane by approximately 0.3 Å,^[23] which leads to the estimated porphyrin–porphyrin distance of 7.5 Å, in agreement with the estimated open geometry shown in Figure 2. Small supplementary energy costs are required to overcome steric constraints and distortions. This cost may explain why the association constant of 2Zn_2 for DABCO is nearly two orders of magnitude smaller than the K_{assoc} of flexible bisporphyrins for DABCO. Similar experiments carried out with the pacman scaffold 1Zn_2 were perturbed by

acid–base equilibrium between DABCO and one hydroxyl group of the calixarene, precluding the determination of $\log K_a$. Titrations of **2Zn₂** or **2H₄** with a more voluminous guest such as C₆₀ led to spectral changes that could not be fitted with a 1:1 receptor/substrate model.

Based on these considerations, it is reasonably assumed that the pacman **2Zn₂** reaches an average porphyrin–porphyrin central core distance that is shorter than 7 Å in pure organic solvents, such as toluene, chloroform and dichloromethane. Thus, the pacman adopts a rather closed conformation. It is worth noting that such a conformation should allow either the binding of coordinating solvents inside the pacman, or the insertion of a flat guest maintained by π -stacking interactions.^[24]

UV/Vis and stationary fluorescence characterisation: The evolution of UV/Vis spectra of both pacman scaffolds **1** and **2** (Figure 4) compared to their 5-ethynyl–OEP precursors supports cofacial geometry. It has been established that parallel interactions between transition dipole moments of two chromophores should lead to absorption band broadenings associated with these moments, and simultaneously to the displacement of the absorption maxima towards higher energy. This blue shift is inversely proportional to the sepa-

ration of the chromophores (i.e., exciton coupling).^[25] Table 1 shows the absorption maximum data and full width at half maximum (FWHM). The Soret bands of **2Zn₂** and

Table 1. Comparison of the position of the Soret band and the FWHM for pacman bisporphyrin scaffolds **1** and **2** (2-methyl-THF, 298 K).

	5-ethynyl–ZnOEP	1Zn₂	2Zn₂	1H₄	2H₄
λ_{\max} [nm]	418	431	418	431	410
FWHM [nm]	15	31	35	31	46

2H₄ are blue-shifted by 13 and 21 nm with respect to those of **1Zn₂** and **1H₄**, respectively. These shifts reinforce our predictions that the porphyrins are closer to each other in the per-alkylated scaffolds **2Zn₂** and **2H₄** than in the dihydroxylated species **1Zn₂** and **1H₄**. Thus, the ability of the pacman scaffold **2** to close is contingent on the per-alkylation of the calixarene's lower-rim.

When compared to the isolated reference chromophore 5-ethynyl–ZnOEP, the blue shifts of the Soret bands of **2Zn₂** and **2H₄** are less than expected for cofacial porphyrins. Two effects are present that oppositely affect the position of the Soret band. As mentioned above, a cofacial porphyrin arrangement induces a blue shift. However, because free rotation of the porphyrins is hindered in the pacman structure, a longer π -conjugation pathway exists in the pacman scaffold (from the porphyrin to the calixarene's phenyl ring) than in 5-ethynyl–ZnOEP. Extended porphyrin conjugation is reflected by red-shifted absorption bands. Therefore, the blue shift resulting from the cofacial arrangement is partially compensated for by the red shift due to extended conjugation. The small hypsochromic shifts of the Soret bands of **1Zn₂** and **2Zn₂** compared to that of 5-ethynyl–ZnOEP are consistent with the hypothesis that two competing effects are present.

In scaffolds **1Zn₂** and **1H₄**, the Soret bands are red-shifted by 13 nm compared to the Soret band of the reference ethynyl–ZnOEP system. These shifts suggest that, in the dihydroxy pacman **1** series, the extended conjugation plays a more dominant role than exciton coupling on the position of the Soret band. As mentioned above, the blue shift resulting from exciton coupling decreases as the interchromophore distance increases. Given that the porphyrins are further apart in the dihydroxylated scaffolds than in the per-alkylated pacman (see introduction), smaller blue shifts are expected for the former than for the latter.

Several reports support our explanation of the observed red shift of the Soret bands in **1Zn₂** and **1H₄**. Anderson described red-shifted absorption bands as the major effect of induced coplanarity when two ethynyl-bridged bisporphyrin strands were assembled into a double-stranded ladder by *fac* coordination of a bidentate ligand.^[26] When the coordination simultaneously forces the cofacial organisation of the porphyrins, a global red shift and a broadening of the Soret band were observed.^[27] In flexible bisporphyrin pacman, similar features were established upon coordination of

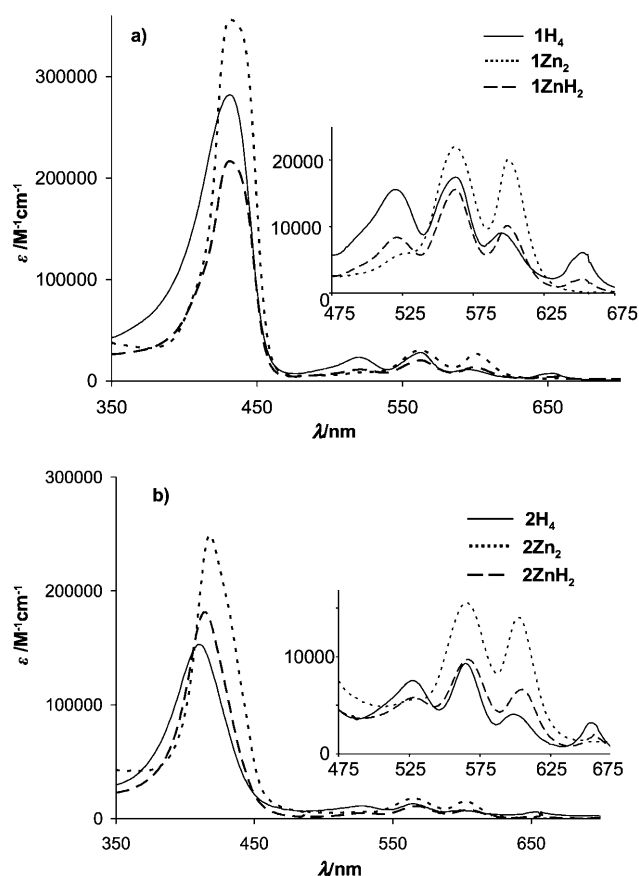


Figure 4. UV/Vis absorption spectra in 2-methyl-THF at 298 K for: a) **1H₄**, **1Zn₂**, **1ZnH₂**; b) **2H₄**, **2Zn₂**, **2ZnH₂**. ϵ values were calculated using the molecular weight of each compound.

DABCO, or when the coplanarity of two porphyrins is caused by steric constraints.^[9–11,13]

The λ_{max} values (in 2-methyltetrahydrofuran, 2-MeTHF) for the Q-bands of each chromophore in dyads **1ZnH₂** and **2ZnH₂**, that is, the (0–0) band at 652 nm in **1H₄** and the (0–1) band at 562 nm for **1Zn₂**, confirm that the ZnP and H₂P chromophores (P=porphyrin derivative) are the singlet energy donor (S₁ D) and acceptor (A), respectively. As seen in Table 2, this D/A attribution is the same for all solvents studied. Steady-state fluorescence spectroscopy also confirms this attribution. The absorption spectrum of **1ZnH₂** exhibits spectral features associated with the absorption bands of both **1H₄** and **1Zn₂**. The spectrum corresponds to nearly the half-sum of the individual spectra of **1H₄** and **1Zn₂**, indicating that interchromophore interactions in the ground state are minimal, or at least not different in homobisporphyrin species than in the dyads.

Although the absorption spectra of each dyad show that the ZnP donor cannot be specifically excited, a qualitative estimation of energy-transfer efficiency from the ZnP donor to the H₂P acceptor can be made. In Figure 5a, for example, at the excitation wavelength of 562 nm, the absorbance of the solution of **1Zn₂** was only half that of the solutions of dyad **1ZnH₂** and of **1H₄**. Thus, in Figure 5a, the decreased emission of the dyad at 611 nm compared to the emission of the zinc donor **1Zn₂** at this wavelength (Figure 5a) signifies efficient energy transfer. The same qualitative conclusion can be drawn from the comparison of the emission spectra the donor **2Zn₂** with that of **2ZnH₂** in Figure 5b.

Nonselective excitation is often found for zinc/free-base porphyrin dyads with similar or identical tetrapyrrolic frameworks. However, when strong spectral overlap exists, quenching and energy transfer can be reliably addressed by measuring fluorescence lifetimes using time-resolved fluorescence studies.^[29] To determine appropriate λ_{em} for time-resolved studies, the emission spectrum of each bis(free-base) and bis-zinc species was measured by using a nonselective excitation wavelength of 562 nm. This wavelength gives the maximum emission intensity for both the donor in the references and the acceptor in the dyads (Figure 5c,d).

The emission spectra of the dyads in Figure 5a,b served primarily to determine the λ_{em} for time-resolved studies.

Time-resolved fluorescence studies: To gain insight into the singlet energy-transfer (SET) process, the fluorescence decay of the ZnP chromophore (donor, D) in each dyad was studied by using its specific emission at 613 nm. Upon excitation at 562 nm, in 2-MeTHF and in toluene, the decreased intensity of the donor's fluorescence at 613 nm at both 298 and 77 K was accompanied by a decrease in τ_{F} (Table 3). For example, in 2-MeTHF at 298 K, $\tau_{\text{F}}(\text{ZnP}) = 0.18 \pm 0.05$ ns and 1.33 ± 0.05 ns for **1ZnH₂** and **1Zn₂**, respectively, confirming the presence of SET. This large difference in τ_{F} suggests an efficient ET that is somewhat surprising for an “open” geometry (which will be established below by DFT). The D–A separation would exceed 10 Å in an open geometry. The second, longer lifetime of 1.67 ns that was detected for **1ZnH₂** was assigned to a partial cone conformer (as shown in Figure 2c), that was present in trace amounts. This second lifetime was not detected in toluene. Therefore, we suggest that the presence of a partial cone conformer in 2-MeTHF is triggered by the perturbation of intramolecular hydrogen bonding at the calixarene's lower rim due to the solvent's heteroatom. Similar observations were reported for energy-transfer dyads in which anthracene and naphthalene chromophores were appended to cyclam spacers.^[28] A conformation change occurred upon metal coordination within the cyclam. This is also supported by the unique short lifetime observed in all solvents upon excitation at 562 nm when the calixarene narrow rim is peralkylated and the conformational equilibrium is suppressed in the case of **2ZnH₂**.

Interestingly, for **1ZnH₂**, the lifetime of ZnP in the partial cone conformer is significantly longer than in **1Zn₂**, despite the fact that the connection between the energy donor and acceptor is the same in both conformers (the number of bonds separating the chromophores is identical). Only one lifetime was detected for **1Zn₂** and **1H₄** in 2-MeTHF; however, trace amounts of the partial cone conformers might be present in both of these references. In 2-MeTHF, the τ_{F} of

Table 2. Absorption band positions in the Q-region and fluorescence band maxima of compounds **1** and **2** ($c = 5 \times 10^{-6}$ M).

	2-methyl-THF		ethanol		toluene	toluene/EtOH (1:1)
	298 K	77 K	298 K	77 K	298 K	298 K
absorption λ_{max} [nm]						
1H₄	520, 562, 595, 652	522, 562, 588, 648	–	–	520, 562, 600, 654	522, 562, 596, 654
1Zn₂	562, 600	562, 600	565, 602	560, 600	558, 596	564, 602
1ZnH₂	522, 562, 598, 654	524, 562, 594, 648	522, 563, 598, 648	522, 561, 598, 646	522, 562, 596, 652	522, 564, 600, 654
2H₄	526, 564, 598, 652	528, 568, 598, 653	–	–	528, 564, 598, 654	528, 566, 598, 652
2Zn₂	566, 602	562, 601	–	–	570, 602	570, 602
2ZnH₂	528, 570, 603, 656	525, 562, 600, 648	–	–	530, 566, 604, 654	530, 566, 604, 656
emission λ_{em} [nm]						
1H₄	656, 725	648, 722	–	–	657, 726	657, 723
1Zn₂	614, 666	606, 655	614, 667	607, 669	612, 667	618, 662
1ZnH₂	611, 658, 725	605, 648, 722	612, 654, 722	607, 647, 721	609, 657, 725	614, 656, 724
2H₄	657, 728	653, 724	–	–	657, 729	658, 730
2ZnH₂	614, 669	613, 672	–	–	618, 679	617, 674
2ZnH₂	613, 657, 727	611, 649, 722	–	–	615, 660, 731	614, 659, 728

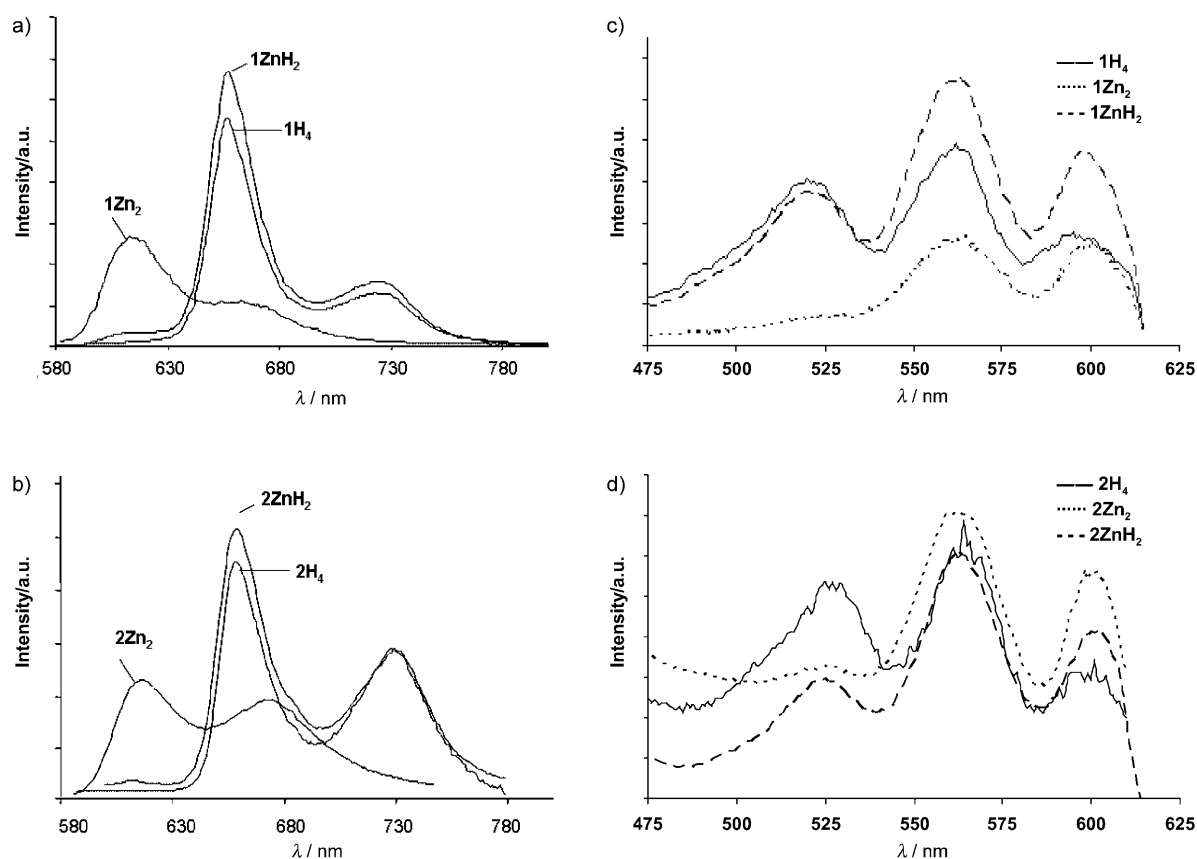


Figure 5. Emission and excitation spectra in 2-MeTHF at 298 K. Qualitative emission spectra (non-selective $\lambda_{\text{ex}}=562$ nm) of: a) **1H₄**, **1Zn₂**, **1ZnH₂**, and b) **2H₄**, **2Zn₂**, **2ZnH₂**. Excitation spectra recorded for maximum emission of the free base at 730 nm for the D–A dyads: c) **1H₄**, **1Zn₂**, **1ZnH₂** and d) **2H₄**, **2Zn₂**, **2ZnH₂**.

Table 3. The parameters τ_F [ns], k_{ET} rates [ns^{-1}] and Φ_{ET} for **1H₄**, **2H₄**, **1Zn₂**, **2Zn₂**, **1ZnH₂** and **2ZnH₂**.^[a]

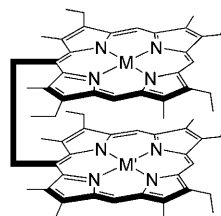
Solvent	<i>T</i> [K]	1H₄		1Zn₂		1ZnH₂				2H₄		2Zn₂		2ZnH₂						
		τ_F	χ^2	τ_0	χ^2	τ_F	$A^{[b]}$	χ^2	k_{ET}	$\Phi_{ET}^{[c]}$	τ_F	χ^2	τ_0	χ^2	τ_F	χ^2	k_{ET}	$\Phi_{ET}^{[c]}$		
2-MeTHF	298	9.79	1.2	1.33	0.90	0.18	1.67	0.93	0.07	1.02	4.8	0.86	6.98	1.40	1.28	0.85	0.25	1.09	3.2	0.88
	77	11.36	0.95	3.04	1.10	0.30	2.81	0.93	0.07	0.6	3.0	0.89	10.90	1.0	2.30	0.91	0.16	1.04	5.8	0.93
C ₇ H ₈	298	5.38	0.95	1.55	0.91	0.17		0.90	5.2	0.89	8.4	0.98	1.19	0.95	0.12	1.08	7.5	0.90		
EtOH	298			2.05	0.95	0.24	2.86	0.60	0.40	0.86	3.7	0.81								
	77			2.78	0.93	0.27		1.05	3.3	0.90	–	–	–	–	–	–	–	–	–	–
C ₇ H ₈ /EtOH (1/1)	298	5.97	1.13	0.93	0.87	0.28	1.50	0.85	0.15	1.00	2.5	0.70	5.45	1.29	1.43	1.10	0.65	0.98	0.8	0.52

[a] All data provided in this table have been obtained by using Timemaster Model TM-3/2003 apparatus from PTI (see Experimental Section for details). The uncertainties were $\pm 10\%$ based on three measurements on different samples. [b] *A* is the pre-exponential factor of each lifetime. [c] Φ_{ET} calculated from the relationship: $\Phi_{\text{ET}} = 1 - (\tau_F/\tau_F^0)$.

the reference compounds **1H₄**, **2H₄**, **1Zn₂** and **2Zn₂** are in the same range as those of reported homo bis-chromophore cofacial systems (**4H₄–8H₄**, Figure 6).^[4] Comparison of τ_F data for **1H₄** (9.79 ns (298 K) and 11.36 ns (77 K)) and **2H₄** (6.98 ns (298 K) and 10.90 ns (77 K), Table 3) with those of **3H₂** (8.70 ns (298 K) and 12.39 ns (77 K)) supports the presence of interporphyrin interactions that promote some *S*₁ excited state deactivation through intramolecular collisions in the fixed cone conformer **2H₄**. Such behaviour is known for cofacial free-base bisporphyrins similar to **4H₄–8H₄** (Figure 6).^[3,4,12] The short lifetime of the ZnP donor in the dyad **1ZnH₂** is remarkable, because it suggests that a very

efficient SET still occurs in a medium that favours the formation of hydrogen bonds and forces an open cone conformation with a *C_{meso-meso}* distance of about 10 Å or more. This unexpectedly fast SET triggered a more detailed comparison with a set of reported dyads.^[4]

The SET process in the series of cofacial donor–acceptor dyads (**4ZnH₂–8ZnH₂**; Figure 6), in which the porphyrin macrocycles are cofacially preorganised by a rigid spacer, were previously reported.^[4] In dyads **5ZnH₂–8ZnH₂**, the same number of chemical bonds separates the donor (ZnP) from the acceptor (H₂P) and the interporphyrin distance is fixed by the nature of the spacer. The distances between the



	$M=Zn; M'=2H$	4ZnH₂	5ZnH₂	6ZnH₂	7ZnH₂	8ZnH₂
k_{ET} [ns ⁻¹] (298 K)		20.8	9.8	6.4	5.0	4.7
k_{ET} [ns ⁻¹] (77 K)		15.4	10.9	7.2	5.0	4.6
$C_{meso}-C_{meso}$ [Å]		3.8	4.32	4.94	5.53	6.33

Figure 6. Chromophore separation based on $C_{meso}-C_{meso}$ distances in reported rigid D–A dyads **4ZnH₂** to **8ZnH₂**, and singlet energy-transfer (SET) rates used for calibration in this work (reference [4]).

C_{meso} atoms vary from 3.80 to 6.33 Å, as established by X-ray data. Two important features regarding the mechanisms of SET were noticed. First, the minimum number of bonds linking the two macrocycles is six for **5ZnH₂–8ZnH₂** and yet the rate for singlet energy transfer varies with the $C_{meso}-C_{meso}$ separation. This means that a through-space energy-transfer process occurs. There was no evidence for through-bond processes and this is probably due to the U-shape structure of the porphyrin–spacer–porphyrin scaffold. These molecules were selected as standards in this work for their structural resemblance with the reported molecules. Therefore, the conclusion drawn in this previous work is that both the Dexter and Förster mechanisms must operate in the reported dyads in which the C···C separations are in the 5–6 Å range. The second feature is that no splitting of the Soret band is noted, meaning that the exciton interactions are minimal. We have used the singlet energy-transfer rate constants measured in dyads **4ZnH₂–8ZnH₂** as a calibration to correlate the D–A separation with the rate of through-space singlet–singlet energy transfer in dyads **1ZnH₂** and **2ZnH₂**.

Estimation of the D–A separations: In the absence of X-ray data, DFT calculations (B3LYP/3-21G*) were used to address the geometry of **1Zn₂**. This compound serves as a model for **1H₄** and **1ZnH₂**. The key DFT results are shown in Figure 7. Pacman **1Zn₂** exhibits an “open” conformation independent of whether an “open” or “closed” starting con-

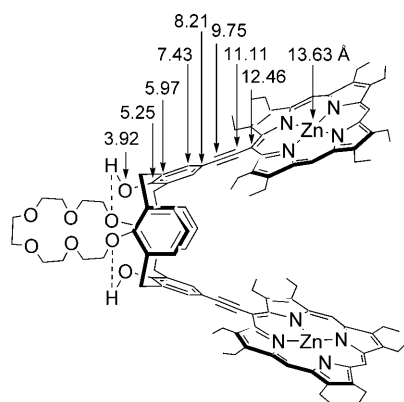


Figure 7. Interatomic distances between identical atoms (symmetry) in the pacman scaffold **1Zn₂** determined by DFT calculations.

formation was set prior to geometry optimisation. The two porphyrin macrocycles remain cofacial throughout the computations. The resulting “gas-phase” structure exhibits two intramolecular hydrogen bonds between the hydroxyl groups at the lower rim and the adjacent oxygen atoms of the crown ether residue. These hydrogen bonds are the driving force for the open conformation, which renders the calix[4]arene ring

somewhat more square in comparison to the known flattened cone geometry. This “open” geometry exhibits a wide range of cofacial O···O, C···C, and Zn···Zn distances (see Figure 7 and also Figure S3 in Supporting Information). The $C_{meso} \cdots C_{meso}$ (12.46 Å) and Zn···Zn (13.63 Å) separations are particularly large in comparison with those of the calibration compounds **4Zn₂–8Zn₂** in Figure 6.

In dyads **1ZnH₂** and **2ZnH₂**, the porphyrin–porphyrin distances are difficult to evaluate confidently from X-ray data of **2Ni₂**,^[10] because the rather flexible nature of the calixarene spacer in **2Ni₂** forbids correlation of the solid-state and solution structures for compounds **2**. Thus, comparison of SET rates in **1ZnH₂** and **2ZnH₂** to those of our references **4ZnH₂–8ZnH₂** was expected to provide a good estimate of donor–acceptor distance. The k_{ET} values can be extracted from τ_F according to $k_{ET} = (1/\tau_F) - (1/\tau_F^0)$,^[2,29] in which τ_F is the fluorescence lifetime (Table 3) of the dyads **1ZnH₂** or **2ZnH₂**, and τ_F^0 is the fluorescence lifetime of references **1Zn₂** or **2Zn₂**. In the references, no SET takes place, but the molecules’ skeletons are nearly identical to those of the dyads. For **1ZnH₂**, SET rates (k_{ET}) of 4.8 ns⁻¹ (298 K), and 3.0 ns⁻¹ (77 K) were obtained. These k_{ET} values compare favourably to those measured for the cofacial dyad **8ZnH₂** (4.7 and 4.6 ns⁻¹) and are slightly slower than those measured for **7ZnH₂** (5.0 and 5.9 ns⁻¹) at 298 and 77 K, respectively.^[4] In toluene at 298 K, k_{ET} is 5.2 ± 0.5 ns⁻¹ for **1ZnH₂**. This value is in the same range as the value of 4.8 ± 0.5 ns⁻¹ in 2-MeTHF at 298 K, indicating that no or little perturbation related to solvent occurs. For **8ZnH₂** and **7ZnH₂**, the $C_{meso}-C_{meso}$ distances are 6.33 and 5.53 Å, respectively.^[4] Based on this comparison, one can deduce that the most probable distance at which SET occurs the most efficiently in **1ZnH₂** is about 5.3 Å. This estimated distance is far from the 12.5 Å suggested in Figure 7 and prompted the search for other possible pathways for energy transfer.

Energy transfer pathways: In both dyads **1ZnH₂** and **2ZnH₂**, the presence of non-conjugated methylene bridges between the calix[4]arene aryl groups is not sufficient to preclude the possibility of through-bond energy transfer; however, the contribution of through-bond energy transfer is assumed to be negligible. Indeed, as discussed later (vide infra), in dyad **1ZnH₂** the lifetime of the donor in the partial cone confor-

mer (1.67 ns) is longer than in the reference donor **1Zn**₂ (1.33 ns). If efficient through-bond energy transfer was operative, one would expect, at the least, a slightly shorter lifetime of the donor compared to the reference donor. Only the lifetime of D in face-to-face (cone) conformers is significantly affected. Second, whereas through-bond interactions play a major role in photoinduced charge-transfer processes,^[30] most photoinduced SETs are usually examined on the basis of through-space interactions through Dexter or Förster mechanisms.^[31] Although the Dexter mechanism corresponds to a two-electron exchange mechanism,^[32] in both the dyads **1ZnH**₂ and **2ZnH**₂ and in the calibration series, the Dexter contribution is mostly through space due to the close proximity of the chromophores. In addition, detailed studies of the dyads **4ZnH**₂–**8ZnH**₂ have shown distance-dependent SET rates in scaffolds with an identical number of bonds. Even though the Förster SET becomes dominant for distances over 5.5 Å, the results can be analysed on the basis of a through-space SET by a mixed contribution of Dexter and Förster mechanisms.

It can be expected that the conjugation of the calixarene spacer with the porphyrin rings through the ethynyl spacers will slightly affect the spin densities on the substituted *meso*-carbon atom. This was confirmed by comparison of the DFT results for the HOMO and LUMO of the chromophores (Figure 8) and the reported calculations for **4–8**. More detailed calculations were performed for a model pacman compound **9Zn**₂ in which the propyl groups of **2Zn**₂ were replaced by methyl groups to save on computation time. Figure 9 shows that in the closed conformer, the frontier orbitals of **9Zn**₂ are built over both chromophores (a complete set of frontier orbitals is provided in the Supporting Information). The rather short interporphyrinic distance in the calculated closed conformer is in full agreement with a significant contribution of a Dexter mechanism in the energy-transfer process in the dyads **4ZnH**₂–**6ZnH**₂. The set of dyads chosen for calibration seems suitable for two major reasons. First, similar variations of the respective contribu-

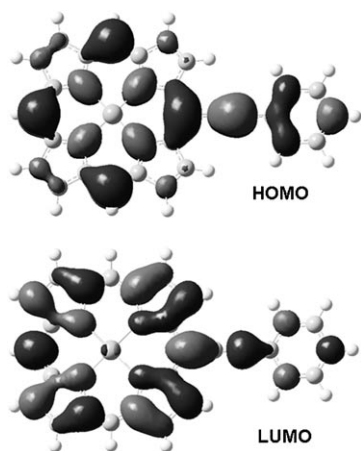


Figure 8. Frontier MOs for Ph–C≡C–(PZn) according to DFT (B3LYP; basis set 3-21G).

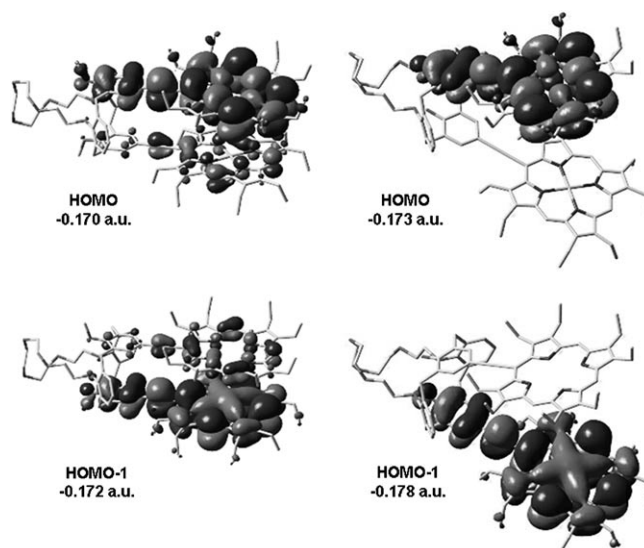


Figure 9. HOMO (top left) and HOMO–1 (bottom left) representations for **9ZnH**₂ as a model of a closed conformation, and HOMO (top right) and HOMO–1 (bottom right) representations for **1ZnH**₂ in the open conformation. Geometries optimised by DFT (B3LYP/3-21G).

tions of Dexter and Förster mechanisms to the energy-transfer process are expected if the contribution of through-bond transfer is neglected. Second, in both the reference dyads and the studied dyads, the D–A pairs are identical within each series. Thus, the relative orientation of transition dipole moments in D and A, and kappa values are nearly constant, rendering the distance versus rate of SET calibration reliable.

Several reports on *meso*-alkynyl porphyrins document π -conjugation as well as efficient communication between the porphyrin ring and ethynyl substituents or linkers.^[33] This is explained by examining the frontier orbitals (HOMO and LUMO), in which an important atomic contribution of the ethynyl groups to these MO's exists.^[34] For the geometry-optimised (DFT; B3LYP/3-21G*) model compound Ph–C≡C–(ZnP) (Figure 8) and for **2Zn**₂ (see Figure S4 in the Supporting Information), the LUMO and HOMO exhibit electronic density that is well distributed over the porphyrin macrocycle and the ethynyl bridge. A reasonable amount of electron density is also present on the phenyl ring, which suggests that through space SET may also occur at the phenyl end of the chromophore.

For distances > 5 Å, the Förster mechanism is dominant for SET.^[4] The ET rate is a function of the distance between D and A according to $k_{\text{ET}} = k_{\text{D}}(R_{\text{F}})^6(1/r)^6$, in which k_{D} is the emission rate constant for D; R_{F} is the Förster radius, that is, the distance at which SET and spontaneous decay of excited D's are equally probable; and r is the D–A distance.^[35,36] This means that as r increases, k_{ET} decreases rapidly. By examining Figure 7, the estimated value of 5.25 Å falls at the calix[4]arene end of the chromophore. Thus, through-space S₁ ET occurs far more rapidly for cofacial atoms located inside the calix[4]arene cavity. This supports a

probable and unprecedented photoprocess occurring “inside” the cavity of the calix[4]arene.

The possible “non-innocent” role of the calixarene spacer in the SET process, induced by intramolecular hydrogen bonds at the lower rim, urged us to study the corresponding propoxy derivatives **2H₄**, **2Zn₂** and **2ZnH₂**. “Gas-phase” geometry optimisation for **9Zn₂** was validated by comparison to the reported X-ray structure of **2Ni₂** (Figure 10).^[10] In the

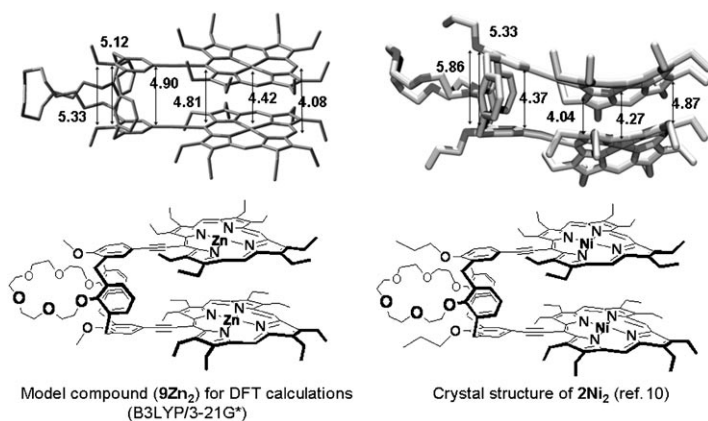


Figure 10. Comparison between significant interatomic distances (in Å) obtained from the computed “gas-phase” geometry of the model compound **9Zn₂** (top left) and the X-ray structure of the related compound **2Ni₂** (top right). For **9Zn₂**, methyl groups were used instead of propyls to save computation time. The average distances of mean planes (porphyrin–ethynyl–phenyl) are 4.78 Å (calculated) and 4.79 Å from X-ray. Local differences are due to packing distortions in the solid state that are ignored in the DFT.

computed model, Zn was employed because this was the metal used in this work. At optimisation, **9Zn₂** adopts a “closed” geometry because no intramolecular hydrogen bonds are possible at the calixarene’s lower rim. The macrocycles are therefore pillared. This calculated conformation bears strong resemblances to the X-ray structure of **2Ni₂**. The average distance of 4.79 Å between mean planes (porphyrin–ethynyl–phenyl) in **2Ni₂** matches the average com-

puted interplanar distance for **9Zn₂** (4.78 Å). The only difference is that some macrocyclic distortions (due to solid state packing) are present for **2Ni₂**. Such behaviour is not uncommon for porphyrins.^[37]

The k_{ET} values at 298 and 77 K for **2ZnH₂** in 2-MeTHF are 3.2 and 5.8 ns^{−1}, respectively. These values are smaller than for dyad **8ZnH₂** with a dibenzothiophene spacer (k_{ET} = 4.7 ns^{−1} at 298 K measured under the same conditions) and higher than that of dyad **7ZnH₂** with a dibenzofuran spacer (k_{ET} = 5.0 ns^{−1} at 77 K). Thus, using the rigid spacer series (**4ZnH₂**–**8ZnH₂**) for calibration, a D⋯A distance of approximately 6 Å can be estimated for the **2ZnH₂** dyad. This distance corresponds to a relaxed closed conformation in which the two chromophores are nearly parallel to each other (based on modelling). Moreover, the k_{ET} value for **2ZnH₂** in toluene is 7.5 ns^{−1}. This rate is somewhat faster than that measured in 2-MeTHF; therefore, the D⋯A separation may be shorter in toluene. This assumption leads to a speculative structure in which the porphyrin macrocycles are closer to each other, resembling the computed structure of **9Zn₂** in Figure 10. This concomitant small increase of the SET efficiency also suggests a shortening of the interporphyrin distance in scaffolds **2** compared to **1**, and is consistent with the conclusions extracted from the above NMR and UV/Vis spectra. Figure 11 summarises the differences between the open and closed conformations of **1ZnH₂** and **2ZnH₂**.

EtOH perturbation on the energy transfers: In the previous discussion, in aprotic solvents, the presence of intramolecular hydrogen bonds between the hydroxyl groups and the crown ether oxygen atoms in **1ZnH₂** imposes the open conformer in this dyad. As mentioned previously, the presence of a heteroatom in 2-MeTHF may provoke the formation of a partial cone conformer. Therefore, the influence of competitive intermolecular hydrogen bonds on the geometry of this molecule, and consequently on its k_{ET} , was studied in EtOH. According to the initial hypothesis, an increased conformational flexibility was expected from the destabilisation of the hydrogen bonds in the cone conformer. For **1ZnH₂**,

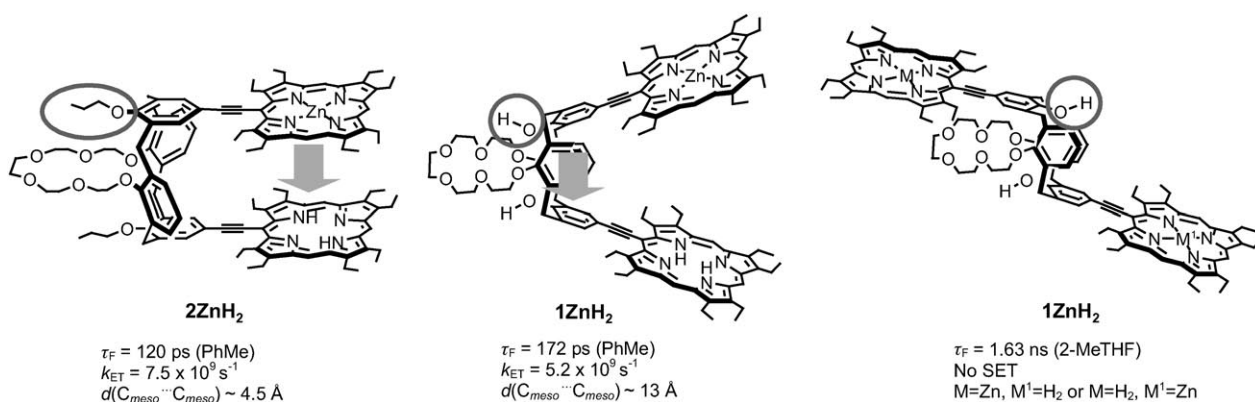


Figure 11. Summary of observed SET processes observed, comparison of k_{ET} data for **2ZnH₂** (left) and **1ZnH₂** (centre) in toluene and **1ZnH₂** (right) in 2-MeTHF. The $d(C \cdots C)$ corresponds to the distance between porphyrin *meso* carbon atoms bearing the ethynyl bridges.

two τ_F values of 0.24 ns (60%) and 2.86 ns (40%) were measured at 298 K. The former value was attributed to the cone conformer and the latter value to the partial cone. The shorter lifetime is now probably associated with a closed cone, due to the concomitant loss of the restrictive hydrogen bonding, and increased hydrophilicity of the medium. Porphyrins are hydrophobic surfaces that are known to aggregate in hydrophilic media. It is thus expected that the two chromophores within the same flexible pacman will tend to closely pack to exclude any solvent molecules from the pacman cavity. The loss of intramolecular hydrogen bonds enhances the spacer's flexibility and increases the amount of partial-cone conformer. The longer lifetime, that was previously observed as a result of trace amounts of partial cone, now significantly contributes (40%) to the decay profile. Upon cooling, the conformational equilibrium between **1ZnH₂** partial cone and cone is significantly shifted to the closed cone conformer, as only one short lifetime is observed (0.27 ns at 77 K).

To show that the contribution of the long-lived species is only observed in the case of incomplete alkylation of the calixarene's narrow rim and in the presence of solvents capable of disrupting the hydrogen bonding at the narrow rim, studies of the per-alkylated dyad **2ZnH₂** in a protic solvent were necessary. Unfortunately, the dyad **2ZnH₂** was insoluble in EtOH. However, it could be dissolved in a 1:1 mixture of toluene and EtOH. In this solvent mixture, only one short-lived species contributed to the decay of **2ZnH₂**. In contrast, one short- and one long-lived species were involved in the decay of dyad **1ZnH₂**, as expected from conclusions previously drawn in this work. Thus, the use of a mixed solvent confirms the assignment of the long lifetime to a partial-cone conformer of dyad **1ZnH₂**. Despite the approximate 5.5 Å distance between the two planes of the phenyl groups bearing the ethynyl–OEP moieties, SET does not take place inside the calixarene, namely between the two nearly parallel aromatic rings. The longer lifetimes that are systematically assigned to a partial cone conformer of **1ZnH₂** are even longer than those of the reference bis-zinc species **1Zn₂**. Two logical reasons explain these longer lifetimes for the partial-cone conformation. First, this partial-cone conformation eliminates deactivating collisions between chromophores. Second, the free rotation of at least one chromophore around the axis of the ethynyl bond decouples the donor or the acceptor from the calixarene platform. This explanation supports the hypothesis that SET occurs inside the cavity when the shortest distance between delocalised frontier orbitals is between two phenyl groups of the calix[4]arene. Such delocalisation is only possible when the confinement of the chromophores in a cofacial environment forces a parallel alignment of the porphyrin rings with the phenyl groups of the calix[4]arene spacer.

Conclusion

A through space SET process was demonstrated for the first time in “flexible” pacman bisporphyrin scaffolds **1ZnH₂** and **2ZnH₂** in which a cofacial arrangement is enforced by a calix[4]arene spacer. Due to the unique “open” and “closed” geometries adopted by the pacman, this process takes place either within the calix[4]arene cavity when the conformation is “open”, or directly between the porphyrin cores in the “closed” form. Without more data, we can only draw conclusions concerning a general trend of the energy-transfer behaviour of bisporphyrin species built around a calixarene spacer. When a partially alkylated calixarene spacer was used (type **1** pacman), the residual hydrogen bonding at the narrow rim could be tuned by solvent interactions. The use of calibration, based on reported time-resolved luminescence studies for rigid pacman architectures, provided an estimation of the D–A distance based on the SET rate.

These new tuneable, through space interactions complete the panel of communications between photo- and electroactive species organised on calixarene platforms for the design of actuators and switches. Although the crown-6 ether at the lower rim of the calix[4]arene contributes to the control of the bowl shape of the calix[4]arene platform, its presence also calls for the development of potential sensing devices. The binding of metal cations at the lower rim should be a remote trigger for changes in the photophysical properties of the pacman bisporphyrin scaffold. Work is in progress to demonstrate this new concept in cofacial bisporphyrin systems.

Experimental Section

Compounds **1Zn₂**, **2H₄**, **2Zn₂**, **3H₂** and **3Zn** were synthesised according to literature procedures.^[13] All reagents and solvents were used as commercial grades, except CH₂Cl₂ and THF, which were distilled respectively over P₂O₅ and sodium/benzophenone, respectively, when necessary. Melting points are uncorrected and were measured on a Kofler heating plate Type 7841. ¹H NMR spectra were recorded on Bruker Avance 500 and Avance 300 spectrometers. Chemical shifts were determined by taking the solvent as a reference: CHCl₃ (7.26 ppm). Coupling constants (*J*) are given in Hz. UV/Vis spectra were performed on a Hewlett Packard 8452 A diode array spectrometer. Chromatography columns were performed on silica gel Merck No. 7734 and alumina Merck No. 1097.

Compound 1H₄: In a flask thoroughly flushed with argon, *meso*-ethynyl–(Zn)OEP (120 mg, 0.193 mmol) and the diiodo(crown-6)dihydroxycalix[4]arene (72 mg, 0.103 mmol) were added to degassed Et₃N (50 mL). Catalytic amounts of [Pd(PPh₃)₂Cl₂] and CuI (10% mol each) were added to the degassed solution. The reaction mixture was stirred at 55 °C for 1 week, and the formation of bis- and monoporphyrin adducts was monitored by TLC (SiO₂, CH₂Cl₂/acetone: 85/15). Additional *meso*-ethynyl–(Zn)OEP (50 mg, 0.08 mmol) and corresponding amounts of [Pd(PPh₃)₂Cl₂] and CuI were added twice after reaction times of 7 and 12 days, to optimise the formation of the bisporphyrin material. After 12 days, no further evolution could be seen by TLC. The solvents were evaporated, and the crude residue was taken in CH₂Cl₂, washed with water, and treated with 10% HCl (aq) to remove the zinc(II) metal core. After washing with water (2×), the crude products were dried by azeotropic distillation with a mixture of toluene and ethanol (2×). The free-base bisporphyrin was purified by column chromatography (SiO₂,

$\text{CH}_2\text{Cl}_2/\text{cyclohexane}$ 9:1) to eliminate the starting material (ethynylporphyrin), butadiene derivative (homocoupling) and other by-products produced by degradation of ethynylporphyrin. The polarity of the eluent was increased by using a gradient of acetone in CH_2Cl_2 (2.5; 5; 7.5; 10; 15; 20; 25 %) to recover two red bands. Fast-moving band: free-base bisporphyrin **1H₄** (46 %), and slower band: **3H₂** (traces). Ultimately, pure free base bisporphyrin **1H₄** was obtained by recrystallisation from a mixture of $\text{CH}_2\text{Cl}_2/\text{MeOH}$ (60 mg, 0.035 mmol, 42 %). ^1H NMR (300 MHz, CDCl_3): δ = 10.11 (s, 4H; H_{meso}), 9.88 (s, 2H; H_{meso}), 8.30 (s, 2H; OH), 7.75 (s, 4H; $\text{H}_{\text{meta(porph)}}$), 7.17 (d, J = 7.4 Hz, 4H; $\text{H}_{\text{meta(H)}}$), 7.01 (t, J = 7.4 Hz, 2H; H_{para}), 4.62 (d, J = 13.5 Hz, 4H; ArCH_2Ar), 4.48 (q, J = 7.7 Hz, 8H; CH_2CH_3), 4.31 (m, 4H; H_{crown}), 4.08 (m (t+q), 34H; CH_2CH_3 + H_{crown}), 3.83 (s, 4H; H_{crown}), 3.63 (d, J = 12.4 Hz, 4H; ArCH_2Ar) 1.90 (t, J = 7.5 Hz, 48H; CH_2CH_3), -2.62 (s, 2H; NH), -2.80 ppm (s, 2H; NH); UV/Vis (CH_2Cl_2): λ_{max} (ϵ) = 431 (356400), 522 (29000), 564 (33100), 592 (15800), 649 nm ($10700\text{ m}^{-1}\text{ cm}^{-1}$); MS (MALDI-TOF): m/z : 1741.098 [M^+]; elemental analysis calcd (%) for $\text{C}_{121}\text{H}_{152}\text{Cl}_6\text{N}_8\text{O}_{12}$ (**1H₄** + $3\text{CH}_2\text{Cl}_2$ + $3\text{H}_2\text{O}$; 2123.3 g mol^{-1}): C 68.58, H 6.98; found: C 68.03, H 6.66.

Compounds 1ZnH₂ and 1Zn₂: In a flask thoroughly flushed with argon, free-base bisporphyrin **1H₄** (70 mg, 0.040 mmol) was dissolved in CH_2Cl_2 (40 mL). The reaction mixture was degassed and heated to reflux. A solution of $\text{Zn}(\text{OAc})_2 \cdot 2\text{H}_2\text{O}$ (10.6 mg, 0.048 mmol) in $\text{CH}_3\text{OH}/\text{CH}_2\text{Cl}_2$ (7 mL of a 1:1 solution) was added dropwise over a period of 1.5 h. The reaction was monitored for the disappearance of the free-base bisporphyrin by UV/Vis spectroscopy and TLC (Al_2O_3 , CH_2Cl_2). After 1.5 h, solvents were evaporated and the residue was dissolved in CH_2Cl_2 and purified by column chromatography (Al_2O_3 , CH_2Cl_2). The red band corresponding to the free-base bisporphyrin **1H₄** was collected first. The second red band, eluted with 1–5 % acetone in CH_2Cl_2 , contained the zinc/free-base bisporphyrin dyad **1ZnH₂**. The last fraction that eluted with 15–20 % acetone in CH_2Cl_2 contained the zinc bisporphyrin **1Zn₂** contaminated by traces of the zinc/free-base bisporphyrin **1ZnH₂**, which could not be detected by TLC. This last fraction was treated with a solution of 10 % HCl, washed three times with H_2O , and dried by azeotrope distillation with toluene and ethanol to regenerate the free-base bisporphyrin **1H₄**. The zinc bisporphyrin **1Zn₂** was subsequently obtained by full metallation of the free-base **1H₄** by using the procedure described above with 10 equivalents of $\text{Zn}(\text{OAc})_2 \cdot 2\text{H}_2\text{O}$ in refluxing methanol for 4 h. The solvent was evaporated, and the residue was dissolved in CH_2Cl_2 , washed with H_2O (3 times), and dried by toluene–ethanol azeotrope distillation.

Characterisation of 1Zn₂: ^1H NMR (300 MHz, $[\text{D}]\text{CHCl}_3$, 25 °C): δ = 10.11 (s, 4H; H_{meso}), 10.03 (s, 2H; H_{meso}), 8.23 (s, 2H; OH), 7.74 (s, 4H; $\text{H}_{\text{meta(porph)}}$), 7.15 (d, J = 7.7 Hz, 4H; $\text{H}_{\text{meta(H)}}$), 6.98 (t, J = 7.3 Hz, 2H; H_{para}), 4.59 (d, J = 12.2 Hz, 4H; ArCH_2Ar), 4.51 (q, J = 6.95 Hz, 8H; CH_2CH_3), 4.25 (m, 4H; H_{crown}), 4.08 (m, 28H; H_{crown} + CH_2CH_3), 3.98 (m, 4H; H_{crown}), 3.91 (m, 4H; H_{crown}), 3.79 (s, 4H; H_{crown}), 3.72 (pseudo t, 2H; H_{crown}), 3.61 (d, J = 13.7 Hz, 4H; ArCH_2Ar), 1.91 ppm (m, 48H; CH_2CH_3); UV/Vis (CH_2Cl_2): λ_{max} (ϵ) = 426 (390500), 556 (34800), 595 nm ($28100\text{ m}^{-1}\text{ cm}^{-1}$); MS (MALDI-TOF): m/z : 1867.86 [M^+]; elemental analysis calcd (%) for $\text{C}_{115}\text{H}_{130}\text{Cl}_2\text{N}_8\text{O}_9\text{Zn}_2$ (**1Zn₂** + CH_2Cl_2 + H_2O): C 70.11, H 6.65; found: C 70.01, H 6.99.

Characterisation of compound 1ZnH₂: ^1H NMR (300 MHz, $[\text{D}]\text{CHCl}_3$, 25 °C): δ = 10.10 (s, 4H; H_{meso}), 10 (s, 1H; H_{meso}), 9.88 (s, 1H; H_{meso}), 8.20 (s, 1H; OH), 8.16 (s, 1H; OH), 7.74 (s, 4H; $\text{H}_{\text{meta(porph)}}$), 7.15 (d, J = 7.6 Hz, 4H; $\text{H}_{\text{meta(H)}}$), 6.98 (t, J = 7.3 Hz, 2H; H_{para}), 4.52 (d+q, J = 11.4, 7.4 Hz, 12H (4+8); ArCH_2Ar + CH_2CH_3), 4.08 (m (t+q), 32H; H_{crown} + CH_2CH_3), 3.93 (m, 4H; H_{crown}), 3.89 (m, 4H; H_{crown}), 3.76 (s, 4H; H_{crown}), 3.69 (pseudo t, 2H; H_{crown}), 3.59 (d, J = 12.4 Hz, 4H; ArCH_2Ar), 1.91 (m, 48H; CH_2CH_3), -2.63 (s, 2H; NH), -2.81 ppm (s, 2H; NH); UV/Vis (CH_2Cl_2): λ_{max} (ϵ) = 427 (358000), 522 (18600), 560 (31200), 594 (20100), 648 nm ($5100\text{ m}^{-1}\text{ cm}^{-1}$); MS (MALDI-TOF): m/z : 1803.95 [M^+]; elemental analysis calcd (%) for $\text{C}_{116}\text{H}_{134}\text{Cl}_4\text{N}_8\text{O}_9\text{Zn}$ (**1Zn₂** + $2\text{CH}_2\text{Cl}_2$ + H_2O): C 69.96, H 6.78; found: C 69.98, H 6.99.

Metallation process for preparing 2ZnH₂: The procedure was identical to that used for the preparation of **1Zn₂** and **1ZnH₂** (vide supra). ^1H NMR (300 MHz, $[\text{D}]\text{CHCl}_3$, 25 °C): δ = 9.03 (s, 1H; H_{meso}), 8.97 (s, 1H; H_{meso}),

8.23 (s, 2H; H_{meso}), 8.12 (s, 2H; H_{meso}), 7.48 (d+d, J = 7.4 Hz, 4H; $\text{H}_{\text{meta(H)}}$), 7.29 (t, J = 7.4 Hz, 2H; H_{para}), 7.06 (s, 2H; $\text{H}_{\text{meta(porph)}}$), 7.02 (s, 2H; $\text{H}_{\text{meta(porph)}}$), 4.66 (m (d+d), J = 11.4 Hz, 4H; ArCH_2Ar), 4.53 (pseudo t, 4H; H_{crown}), 4.25 (pseudo t, 4H; H_{crown}), 4.11 (pseudo q, 4H; CH_2CH_3), 4.00 (pseudo q, 4H; CH_2CH_3), 3.91 (m, 4H; H_{crown}), 3.83 (m, 16H; H_{crown} + CH_2CH_3), 3.73 (pseudo q, 4H; CH_2CH_3), 3.46 (d+d, J = 12.4 Hz, 4H; ArCH_2Ar), 3.29 (m (q+q), 8H; CH_2CH_3), 3.15 (m, 8H; $\text{OCH}_2\text{CH}_2\text{CH}_3$ + CH_2CH_3), 2.08 (m, 4H; $\text{OCH}_2\text{CH}_2\text{CH}_3$), 1.69 (m (t+t), J = 7.8 Hz, 12H; CH_2CH_3), 1.46 (m, 36H; CH_2CH_3), 1.21 (m, 6H; $\text{OCH}_2\text{CH}_2\text{CH}_3$), -0.87 (s, 1H; NH), -1.28 nm (s, 1H; NH); UV/Vis (toluene): λ_{max} (ϵ) = 415 (139500), 531 (5900), 572 (8500), 608 nm ($6600\text{ m}^{-1}\text{ cm}^{-1}$); MS (FAB⁺): m/z : 1888.01 [M^+].

Note: Elemental analysis of peralkylated pacman **2** derivatives were obtained but could not be fitted with the calculated species using an integer number of water molecules, whereas the hydroxylated scaffolds **1** always contained at least one water molecule. This is consistent with a tight interaction of water with the lower rim of the calixarene when only partially alkylated. The water molecule in scaffold **2** was labile enough to be partly removed upon drying. Analyses were thus performed on each sample used for physical measurements.

Time-resolved luminescence studies: Emission and excitation spectra were obtained using a double monochromator Fluorolog 2 instrument from Spex. Fluorescence lifetimes were measured on a Timemaster Model TM-3/2003 apparatus from PTI. The source was a nitrogen laser equipped with a high-resolution dye laser (FWHM \approx 1500 ps) and all the fluorescence lifetimes reported in this work were obtained from deconvolution and distribution lifetime analysis. The uncertainties were \pm 10 % based on three measurements on different samples. Some lifetimes were shorter than 100 ps (from deconvolution). For short fluorescence lifetimes (i.e., on the 100 ps timescale), controls were performed using a ps laser system (FWHM = 10 ps) located at the University of Ottawa (Prof. Scaiano), but the values reported in the tables were collected on the Timemaster equipment. The uncertainty is \pm 50 ps in this work. Details are provided in reference [4]. All samples were prepared under an inert atmosphere (in a glove box, $\text{P}(\text{O}_2)$ < 1–3 ppm) by dissolution of the different compounds in 2-MeTHF in 1 cm^3 quartz cells equipped with a septum (298 K) or in standard 5 mm NMR tubes (77 K). Three different measurements (i.e. different solutions) were performed for each photo-physical datum (lifetimes). The UV/Vis spectra were measured on HP 8452 A diode array spectrophotometer in Sherbrooke, and on an Agilent 8453E diode array UV/Vis spectrometer in Strasbourg.

Computer modelling: The calculations were performed with the Density Functional Theory (DFT) approximation using the commercially available Gaussian 03 software.^[38] The hybrid B3LYP exchange correlation function was considered due to the high accuracy of the ensued results,^[39–41] with the 3-21G* as the basis set.^[42] All computations were performed without symmetry constraint.

Association constant measurement: A solution of **2Zn₂** ($c = 3 \times 10^{-6}\text{ M}$; 2 mL, $6 \times 10^{-6}\text{ mmol}$) in toluene was titrated with a $6 \times 10^{-4}\text{ M}$ solution of diazabicyclooctane (DABCO) in toluene at 298 K. Aliquots of 1 μL (0.1 equivalents, 0.6 mmol) of DABCO were added successively from 0 to 1 equivalent. Higher substrate/receptor ratios (1.5, 2.0, 3.0, 5.0, 10.0, 25, and 50) were then reached until no further changes could be detected in the spectrum. Data were then treated using the software SPECFIT on the basis of a 1:1 complex to afford unequivocally a $\log K_a = 6.39 \pm 0.05$.^[43]

Acknowledgements

G.P., J.A.W. and J.W. gratefully acknowledge the CNRS and ULP for financial support. The Ministère de l'Éducation Nationale, Recherche et Technologie (MENRT) is acknowledged for a Ph.D. fellowship (G.P.) and cooperative PICS grant #3183. P.D.H. thanks the Natural Sciences and Engineering Research Council of Canada (NSERC) for generous funding. The authors thank Mr. Shawkat Mohammed Aly (Université de Sherbrooke) for the measurements of some fluorescence lifetimes.

- [1] a) J. Deisenhofer, O. Epp, K. Miki, R. Huber, H. Michel, *J. Mol. Biol.* **1984**, *180*, 385; b) R. Huber, *Angew. Chem.* **1989**, *101*, 849; *Angew. Chem. Int. Ed. Engl.* **1989**, *28*, 848.
- [2] a) P. D. Harvey, in *The Porphyrin Handbook*, Vol. 18 (Eds.: K. M. Kadish, K. M. Smith, R. Guilard), Academic Press, San Diego, **2003**, Chapter 113; b) J. A. Wytko, J. Weiss, in *N₄-Macrocyclic Metal Complexes* (Eds.: J. Zagal, F. Bedioui, J. P. Dodelet), Springer, Berlin, **2006**, pp. 603–712.
- [3] S. Faure, C. Stern, E. Espinosa, J. Douville, R. Guilard, P. D. Harvey, *Chem. Eur. J.* **2005**, *11*, 3469.
- [4] S. Faure, C. Stern, R. Guilard, P. D. Harvey, *J. Am. Chem. Soc.* **2004**, *126*, 1253.
- [5] a) G. Proni, G. Pescitelli, X. Huang, K. Nakanishi, N. Berova, *J. Am. Chem. Soc.* **2003**, *125*, 12914; b) V. V. Borovkov, I. Fujii, A. Muranaka, G. A. Hembury, T. Tanaka, A. Ceulemans, N. Kobayashi, Y. Inoue, *Angew. Chem.* **2004**, *116*, 5597; *Angew. Chem. Int. Ed.* **2004**, *43*, 5481; c) V. V. Borovkov, G. A. Hembury, Y. Inoue, *J. Org. Chem.* **2005**, *70*, 8743; d) L. Valli, S. Casilli, L. Giotto, B. Pignataro, S. Conoci, V. V. Borovkov, Y. Inoue, S. Sortino, *J. Phys. Chem. B* **2006**, *110*, 4691; e) T. Ema, N. Ouchi, T. Doi, T. Korenaga, T. Sakai, *Org. Lett.* **2005**, *7*, 3985.
- [6] a) P. Ballester, A. Costa, P. M. Deya, A. Frontera, R. M. Gomila, A. I. Oliva, J. K. M. Sanders, C. A. Hunter, *J. Org. Chem.* **2005**, *70*, 6616; b) L. Baldini, P. Ballester, A. Casnati, R. M. Gomila, C. A. Hunter, F. Sansone, R. Ungaro, *J. Am. Chem. Soc.* **2003**, *125*, 14181.
- [7] G. Hungerford, M. van der Auweraer, J.-C. Chambron, V. Heitz, J.-P. Sauvage, J.-L. Pierre, D. Zurita, *Chem. Eur. J.* **1999**, *5*, 2089.
- [8] M. Linke-Schaetzel, C. E. Anson, A. K. Powell, G. Buth, E. Palomares, J. D. Durrant, T. S. Balaban, J.-M. Lehn, *Chem. Eur. J.* **2006**, *12*, 1931.
- [9] D. Jokic, Z. Asfari, J. Weiss, *Org. Lett.* **2002**, *4*, 2129.
- [10] G. Pognon, C. Boudon, K. Schenk, M. Bonin, B. Bach, J. Weiss, *J. Am. Chem. Soc.* **2006**, *128*, 3488.
- [11] D. Jokic, C. Boudon, G. Pognon, M. Bonin, K. Schenk, M. Gross, J. Weiss, *Chem. Eur. J.* **2005**, *11*, 4199.
- [12] J.-P. Tremblay-Morin, S. Faure, D. Samar, C. Stern, R. Guilard, P. D. Harvey, *Inorg. Chem.* **2005**, *44*, 2836.
- [13] G. Pognon, J. A. Wytko, J. Weiss, *Org. Lett.* **2007**, *9*, 785.
- [14] V. A. Azov, A. Schlegel, F. Diederich, *Bull. Chem. Soc. Jpn.* **2006**, *79*, 1926.
- [15] a) A. Vigalok, T. M. Swager *Adv. Mater.* **2002**, *14*, 368; b) H.-H. Yu, B. Xu, T. M. Swager, *J. Am. Chem. Soc.* **2003**, *125*, 1142.
- [16] V. Wing-Wah Yam, K. L. Cheung, L. H. Yuan, K. M.-C. Wong, K.-K. Cheung, *Chem. Commun.* **2000**, 1513.
- [17] J. Casanovas, D. Zanuy, C. Alemán, *Angew. Chem.* **2006**, *118*, 1121; *Angew. Chem. Int. Ed.* **2006**, *45*, 1103, and references cited.
- [18] a) D. Zanuy, J. Casanovas, C. Alemán, *J. Phys. Chem. B* **2006**, *110*, 9876; b) C. Alemán, D. Zanuy, J. Casanovas, *J. Org. Chem.* **2006**, *71*, 6952.
- [19] P. D. Harvey, C. Stern, C. P. Gros, R. Guilard, *Coord. Chem. Rev.* **2007**, *251*, 401.
- [20] S. Yagi, I. Yonekura, M. Awakura, M. Ezoe, T. Takagishi, *Chem. Commun.* **2001**, 557.
- [21] R. M. Gomila, C. Garau, A. Frontera, D. Quinonero, P. Ballester, A. Costa, P. M. Deya, *Tetrahedron Lett.* **2004**, *45*, 9387.
- [22] a) S. Bhattacharya, T. Shimawaki, X. Peng, A. Ashokkumar, S. Aonuma, T. Kimura, N. Komatsu, *Chem. Phys. Lett.* **2006**, *430*, 435; b) D. Sun, F. S. Tham, C. A. Reed, L. Chaker, P. D. W. Boyd, *J. Am. Chem. Soc.* **2002**, *124*, 6604.
- [23] B. Cheng, W. R. Scheidt, *Inorg. Chim. Acta* **1995**, *237*, 5.
- [24] a) S. Yagi, M. Ezoe, I. Yonekura, T. Takagishi, H. Nakazumi, *J. Am. Chem. Soc.* **2003**, *125*, 4068; b) M. J. Gunter, M. R. Johnston, *Tetrahedron Lett.* **1992**, *33*, 1771.
- [25] a) M. Kasha, H. R. Rawls, M. A. El-Bayoumi, *Pure Appl. Chem.* **1965**, *11*, 371; b) M. Kasha, *Radiat. Res.* **1963**, *20*, 55; c) C. Hunter, J. K. M. Sanders, A. J. Stone, *Chem. Phys.* **1989**, *133*, 395; d) J. M. Ribb, J. M. Boffill, J. Crusats, R. Rubires, *Chem. Eur. J.* **2001**, *7*, 2733.
- [26] a) M. U. Winters, E. Dahlstedt, H. E. Blades, C. J. Wilson, M. J. Frampton, H. L. Anderson, B. Albinsson, *J. Am. Chem. Soc.* **2007**, *129*, 4291; b) K. J. McEwan, P. A. Fleitz, J. E. Rogers, J. E. Slagle, D. G. McLean, H. Kadas, M. Katterle, I. M. Blake, H. L. Anderson, *Adv. Mater.* **2004**, *16*, 1933.
- [27] F. C. Grozema, C. Houarnier-Rassin, P. Prins, L. D. A. Siebbeles, H. L. Anderson, *J. Am. Chem. Soc.* **2007**, *129*, 13370.
- [28] E. G. Moore, P. V. Bernhardt, M. J. Riley, T. A. Smith, *Inorg. Chem.* **2006**, *45*, 51.
- [29] B. Valeur, *Molecular Fluorescence: Principles and Applications*, Wiley-VCH, Weinheim, **2002**.
- [30] H. Oevering, J. W. Verhoeven, M. N. Paddon-Row, J. M. Warman, *Tetrahedron* **1989**, *45*, 4751.
- [31] For an example of slower SET rates with a reduced number of bonds between D and A see: X. Wang, D. H. Levy, M. B. Rubin, S. Speiser, *J. Phys. Chem. A* **2000**, *104*, 6558; for a detailed discussion demonstrating that distance and kappa are the rate-determining factors in energy-transfer processes see: T. S. Balaban, N. Berova, C. M. Drain, R. Hauschild, X. Huang, H. Kalt, S. Lebedkin, J.-M. Lehn, F. Nifaitis, G. Pescitelli, V. I. Prokhorenko, G. Riedel, G. Smeureanu, J. Zeller, *Chem. Eur. J.* **2007**, *13*, 8411.
- [32] a) H. Oevering, J. W. Verhoeven, M. N. Paddon-Row, E. Cotsaris, N. S. Hush, *Chem. Phys. Lett.* **1988**, *143*, 488; b) G. L. Closs, P. Piotrowiak, J. M. MacInnis, G. R. Fleming, *J. Am. Chem. Soc.* **1988**, *110*, 2652; c) G. L. Closs, M. D. Johnson, J. D. Miller, P. Piotrowiak, *J. Am. Chem. Soc.* **1989**, *111*, 3751.
- [33] a) M. Kawao, H. Ozawa, H. Tanaka, T. Ogawa, *Thin Solid Films* **2006**, *499*, 23; b) T. V. Duncan, K. Susumu, L. E. Sinks, M. J. Therien, *J. Am. Chem. Soc.* **2006**, *128*, 9000; c) H. S. Cho, D. H. Jeong, M.-C. Yoon, Y. H. Kim, Y.-R. Kim, D. Kim, S. C. Jeoung, S. K. Kim, N. Aratani, H. Shinmori, A. Osuka, *J. Phys. Chem. A* **2001**, *105*, 4200; d) J. J. Piet, P. N. Taylor, B. R. Wegewijs, H. L. Anderson, A. Osuka, J. M. Warman, *J. Phys. Chem. B* **2001**, *105*, 97.
- [34] Z. Wang, P. N. Day, R. Pachter, *J. Chem. Phys.* **1998**, *108*, 2504.
- [35] T. Förster, *Naturwissenschaften* **1946**, *33*, 166.
- [36] T. Förster, *Ann. Phys.* **1948**, *2*, 55.
- [37] a) W. R. Scheidt, Y. Lee, *Struct. Bonding (Berlin)* **1987**, *64*, 1; b) E. F. Meyer, *Acta Crystallogr. Sect. B* **1972**, *28*, 2162.
- [38] Gaussian 03 (Revision C.02), M. J. Frisch, G. W. Trucks, H. B. Schlegel, G. E. Scuseria, M. A. Robb, J. R. Cheeseman, J. A. Montgomery Jr., T. Vreven, K. N. Kudin, J. C. Burant, J. M. Millam, S. S. Iyengar, J. Tomasi, V. Barone, B. Mennucci, M. Cossi, G. Scalmani, N. Rega, G. A. Petersson, H. Nakatsuji, M. Hada, M. Ehara, K. Toyota, R. Fukuda, J. Hasegawa, M. Ishida, T. Nakajima, Y. Honda, O. Kitao, H. Nakai, M. Klene, X. Li, J. E. Knox, H. P. Hratchian, J. B. Cross, C. Adamo, J. Jaramillo, R. Gomperts, R. E. Stratmann, O. Yazyev, A. J. Austin, R. Cammi, C. Pomelli, J. W. Ochterski, P. Y. Ayala, K. Morokuma, G. A. Voth, P. Salvador, J. J. Dannenberg, V. G. Zakrzewski, S. Dapprich, A. D. Daniels, M. C. Strain, O. Farkas, D. K. Malick, A. D. Rabuck, K. Raghavachari, J. B. Foresman, J. V. Ortiz, Q. Cui, A. G. Baboul, S. Clifford, J. Cioslowski, B. B. Stefanov, G. Liu, A. Liashenko, P. Piskorz, I. Komaromi, R. L. Martin, D. J. Fox, T. Keith, M. A. Al-Laham, C. Y. Peng, A. Nanayakkara, M. Challacombe, P. M. W. Gill, B. Johnson, W. Chen, M. W. Wong, C. Gonzalez, J. A. Pople, Gaussian, Inc., Pittsburgh, PA, **2004**.
- [39] A. D. Becke, *J. Chem. Phys.* **1993**, *98*, 5648.
- [40] C. Lee, W. Yang, R. G. Parr, *Phys. Rev. B* **1988**, *37*, 785.
- [41] B. Miehlisch, A. Savin, H. Stoll, H. Preuss, *Chem. Phys. Lett.* **1989**, *157*, 200.
- [42] a) K. D. Dobbs, W. J. Hehre, *J. Comput. Chem.* **1986**, *7*, 359; b) K. D. Dobbs, W. J. Hehre, *J. Comput. Chem.* **1987**, *8*, 861; c) K. D. Dobbs, W. J. Hehre, *J. Comput. Chem.* **1987**, *8*, 880.
- [43] We are grateful to Dr. M. Elhabiri from the Laboratory of Physical Biochemistry for treatment of the data provided in the Supporting Information (Figure S1.).

Received: February 18, 2008

Revised: September 4, 2008

Published online: November 26, 2008